Chin. Phys. B Vol. 19, No. 5 (2010) 050518

Kinetic Ising model in a time-dependent oscillating external magnetic field: effective-field theory*

Bayram Deviren[a)b)], Osman Canko[c)], and Mustafa Keskin[c)†]

[a)] *Institute of Science, Erciyes University, 38039 Kayseri, Turkey*
[b)] *Department of Physics, Nevsehir University, 50300 Nevsehir, Turkey*
[c)] *Department of Physics, Erciyes University, 38039 Kayseri, Turkey*

(Received 1 September 2009; revised manuscript received 4 September 2009)

Recently, Shi *et al.* [2008 *Phys. Lett.* A **372** 5922] have studied the dynamical response of the kinetic Ising model in the presence of a sinusoidal oscillating field and presented the dynamic phase diagrams by using an effective-field theory (EFT) and a mean-field theory (MFT). The MFT results are in conflict with those of the earlier work of Tomé and de Oliveira, [1990 *Phys. Rev.* A **41** 4251]. We calculate the dynamic phase diagrams and find that our results are similar to those of the earlier work of Tomé and de Oliveira; hence the dynamic phase diagrams calculated by Shi *et al.* are incomplete within both theories, except the low values of frequencies for the MFT calculation. We also investigate the influence of external field frequency (ω) and static external field amplitude (h_0) for both MFT and EFT calculations. We find that the behaviour of the system strongly depends on the values of ω and h_0.

Keywords: kinetic Ising model, effective-field theory, mean-field theory
PACC: 0550, 0570F, 6460H, 7510H

1. Introduction

In a recent paper, Shi *et al.*[1] studied the kinetic Ising model under a time-dependent oscillating field within an effective-field theory (EFT) with correlations and mean-field theory (MFT). Especially, they investigated the temperature dependencies of the dynamic order parameter and the dynamic correlations. From these investigations, they obtained the dynamic phase transition (DPT) points and presented the dynamic phase diagrams. In recent years, the dynamic phase transition has become an interesting field of research in magnetic model systems, theoretically (see Refs. [2]–[14] and references therein), and in ultrathin ferromagnetic films, ferroic systems, superconductors and polymers, experimentally (see Refs. [15]–[18] and references therein).

Shi *et al.*[1] investigated the temperature dependencies of the dynamic order parameter, hysteresis loop area and correlation. From these investigations, they obtained the DPT points and presented the dynamic phase diagrams. We have realized that the MFT results are in conflict with those of the earlier work of Tomé and de Oliveira[2] for $\omega \geq 0.60$, where ω is the frequency of the external magnetic field. The main conflict is that at low reduced temperatures, there is a range of values of h/zJ in which the paramagnetic (P) and the ferromagnetic (F) phases or regions coexist, which are called the coexistence region or the mixed phase (F+P) for $\omega \geq 0.60$. The F+P mixed phase is separated from F and P phases by the first-order phase lines, hence the mixed phase was not obtained by Shi *et al.*[1] (see comparison between Fig. 3 of Ref. [1] and Figs. 5 and 6 of Ref. [2]). They did not present the time variation of the average magnetization in order to find the phases in the system and they did not study the influence of the external magnetic field frequency and static external magnetic field for both MFT and EFT calculations either.

In this work, first we investigate the time dependence of average magnetization to find the phases in the system in detail. Then, we investigate the behaviour of the average magnetization in a period or the dynamic magnetization as a function of reduced temperature to characterize the nature (continuous and discontinuous) of the transition as well as to obtain the DPT points. We find that the calculated dynamic phase diagrams in Ref. [1] are incomplete within the MFT and the EFT. We also investigate the effects of the external magnetic field frequency, the oscillating

*Project supported by the Scientific and Technological Research Council of Turkey (TÜBİTAK) (Grant No. 107T533) and the Erciyes University Research Funds (Grant Nos. FBA-06-01 and FBD-08-593).
†Corresponding author. E-mail: keskin@erciyes.edu.tr
© 2010 Chinese Physical Society and IOP Publishing Ltd

and static external magnetic field for both the MFT and the EFT calculations.

The structure of the rest of this work is as follows. In Section 2, we briefly give the basic frameworks of the MFT and the EFT. The detailed numerical results and discussion are presented in Section 3, followed by a brief summary.

2. Formulation

A kinetic Ising model with N spins is described by the Hamiltonian given as

$$H = -\sum_{\langle ij\rangle} J_{ij}\, S_i\, S_j - h(t)\left(\sum_i S_i\right), \qquad (1)$$

where S_i takes the values ± 1 at each site i of a lattice; $\langle ij\rangle$ indicates the summation over all pairs of the nearest neighbour sites; J_{ij} represents the spin–spin interaction strength between sites i and j; for simplicity, all J_{ij} are taken to be equal to a constant $J > 0$; $h(t)$ is the time-dependent external field given by $h(t) = h_0 \sin(\omega t)$. The system is in contact with an isothermal heat bath at temperature $T_{\rm abs}$.

The system evolves according to a Glauber-type stochastic process at a rate of $1/\tau$ transitions per unit time. Applying the Glauber transition rate, the mean-field dynamical equation of motion for the kinetic Ising system was found to be,[1,2]

$$\tau \frac{\mathrm{d}}{\mathrm{d}t}\langle S_i\rangle = -\langle S_i\rangle + \left\langle \tanh\left[\beta\left(h(t) + J\sum_j S_j\right)\right]\right\rangle, \qquad (2)$$

where $\beta = 1/k_{\rm B}T_{\rm abs}$, $T_{\rm abs}$ is the absolute temperature and $k_{\rm B}$ is the Boltzmann factor. This dynamic equation can be written in terms of a mean-field approach; hence, the mean-field dynamical equation of the system in the presence of a time-varying field is

$$\frac{\mathrm{d}}{\mathrm{d}t}M = -M + \tanh\left(\frac{M+h}{T}\right), \qquad (3)$$

where $M = < S_i >$ and the Boltzmann constant is set to be unity and $\tau = 1$, the temperature T and the external field h are measured in units of zJ (z is the coordination number).

Now, we use the EFT with correlations to obtain the dynamical equation of motion for the kinetic Ising system. This method was first introduced by Honmura and Kaneyoshi[19] and Kaneyoshi *et al.*,[20] which is a more advanced method of dealing with Ising systems than the MFT, because it considers more correlations. Within the framework of the EFT, one finds that

$$M = \langle S_i\rangle = \left\langle \prod_{i=1}^{z} \left[\cosh(J\nabla) + 2\, S_i\, \sinh(J\nabla)\right]\right\rangle \times\ f(x+h)|_{x=0}\,, \qquad (4)$$

$\nabla = \partial/\partial x$ is a differential operator; $z = 4$ is for the square lattice and $z = 6$ for the simple cubic lattice. The function $f(x+h)$ is

$$f(x+h) = \tanh\left[\beta\,(x+h)\right]. \qquad (5)$$

Equation (4) is also exact and valid for any lattice. If we try to exactly treat all the spin–spin correlations for that equation, the problem quickly becomes intractable. A first obvious attempt to deal with it is to ignore correlations; the decoupling approximation

$$\langle S_i\, S_{i'} \ldots S_{i^n}\rangle \cong \langle S_i\rangle \langle S_{i'}\rangle \ldots \langle S_{i^n}\rangle \qquad (6)$$

with $i \neq i' \neq \ldots \neq i^n$ has been introduced within the EFT with correlations.[19,21,22] In fact, the approximation corresponds essentially to the Zernike approximation[23] in the bulk problem, and has been successfully applied to a great number of magnetic systems including the surface problems.[19,21,22,24] On the other hand, in the MFT, all the correlations, including the self-correlations, are neglected. Based on this approximation, Eq. (4) reduce to

$$M = \left[\cosh(J\nabla) + 2\,M\,\sinh(J\nabla)\right]^z\ f(x+h)|_{x=0}\,. \qquad (7)$$

For the square lattice $z = 4$, expanding Eq. (7), after some manipulations the dynamic equation of motion for the magnetization reads[1]

$$\frac{\mathrm{d}}{\mathrm{d}t}M = -M + a_0 + a_1 M + a_2 M^2 + a_3 M^3 + a_4 M^4, \qquad (8)$$

for the simple cubic lattice $z = 6$, it becomes

$$\frac{\mathrm{d}}{\mathrm{d}t}M = -M + b_0 + b_1 M + b_2 M^2 + b_3 M^3 + b_4 M^4 + b_5 M^5 + b_6 M^6. \qquad (9)$$

The coefficients a_i (i = 0–4) and b_j (j = 0–6) can be easily calculated from a mathematical relation $\exp(\alpha\nabla)\, f(x) = f(x+\alpha)$, where $\nabla = \partial/\partial x$ is a differential operator. These coefficients are given in the Appendix.

The dynamic order parameter or dynamic magnetization as the time-averaged magnetization over a period of the oscillating magnetic field is given as

$$Q = \frac{\omega}{2\pi} \oint M(t) \mathrm{d}t. \tag{10}$$

On the other hand, the hysteresis loop area is

$$A = -\oint M(t) \mathrm{d}h = -h_0 \omega \oint M(t) \cos(\omega t) \mathrm{d}t, \tag{11}$$

which corresponds to the energy loss due to the hysteresis. The dynamic correlation is calculated to be

$$\begin{aligned} C &= \frac{\omega}{2\pi} \oint M(t)\, h(t) \mathrm{d}t \\ &= \frac{\omega h_0}{2\pi} \oint M(t) \sin(\omega t) \mathrm{d}t. \end{aligned} \tag{12}$$

We should also mention that in the numerical calculations, the hysteresis loop area A and the dynamic correlation C are also measured in units of zJ. In the next section we will give the numerical results of these equations.

3. Numerical results and discussions

First, we study time variations of the average order parameter in order to find the phases in the systems. The stationary solutions of Eqs. (3), (8) and (9) will be a periodic function of ωt with period 2π, that is, $M(\omega t + 2\pi) = M(\omega t)$. Moreover, they can be one of two types according to whether they have the property

$$M(\omega t + \pi) = -M(\omega t). \tag{13}$$

A solution that satisfies Eq. (13) is called a symmetric solution which corresponds to a P solution. In this solution, the average magnetization $M(\omega t)$ oscillates around the zero value and is delayed with respect to the external field. The second type of solution which does not satisfy Eq. (13) is called nonsymmetric solution that corresponds to a F solution. In this case the average magnetization does not follow the external magnetic field any more; instead of oscillating around a zero value, it oscillates around a nonzero value. These facts are seen explicitly from the solutions of Eqs. (3), (8) and (9), obtained by using the Adams–Moulton predictor corrector method for a given set of parameters and initial values. Figure 1 shows the solutions for only Eqs. (8) and (9). From the Fig. 1, one can see that three different solutions, namely the P solution, the F, solution and the coexisting solution (F+P) in which the F and the P solutions coexist, exist in the system. In Fig. 1(a) only the symmetric solution is always obtained, hence we have a P solution, but in Fig. 1(b) only the nonsymmetric solution is found, therefore we have a F solution. Both solutions do not depend on the initial values. On the other hand, in Fig. 1(c) both symmetric and nonsymmetric solutions exist in the system, hence we have the coexisting solution or mixed phase (F+P). Therefore, we find that the F+P mixed phase always exists in the system within the EFT for all ω values. We also obtain time variation of the average magnetization within the MFT and find exactly the same behaviour as that within the EFT as shown in

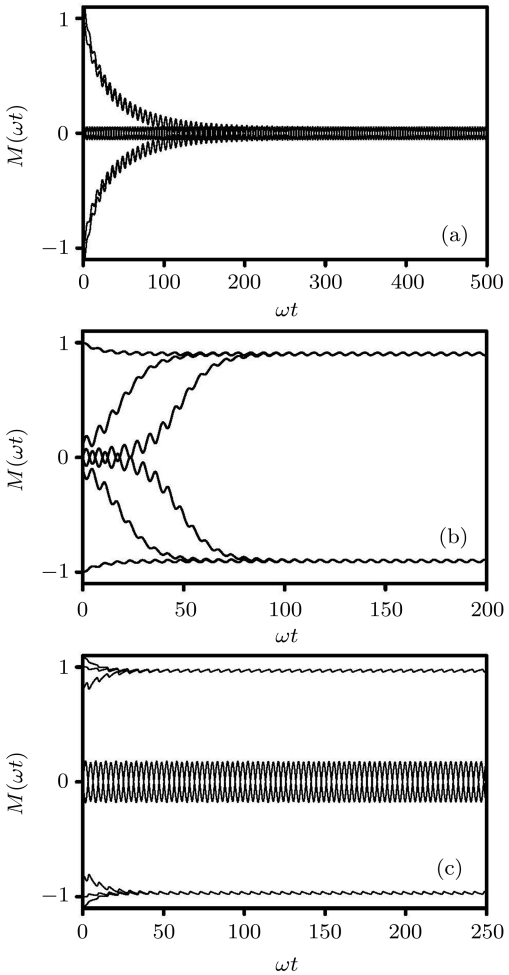


Fig. 1. Time variations of average magnetization (M) for P phase, $\omega = 1.0$, $h/zJ = 0.50$, $T/zJ = 0.80$ and $z = 4$ (a); F phase, $\omega = 0.5$, $h/zJ = 0.25$, $T/zJ = 0.25$ and $z = 4$ (b); F+P phase, $\omega = 1.0$, $h/zJ = 0.70$, $T/zJ = 0.05$ and $z = 4$ (c).

Fig. 1. We have not presented the figures of the MFT calculation in order to avoid giving an unacceptable

number of figures and duplications of explanations. Thus, the F+P mixed phase exists in the MFT for $w \geq 0.60$ and in the EFT for all w values. We should also mention that the P+F mixed phase exists in the system within the EFT with correlations in which this mixed phase was not obtained by Shi *et al.*[1]

We also study the behaviours of the average order parameter in a period or the dynamic magnetization (Q), hysteresis loop area (A/zJ) and correlation (C/zJ), each as a function of the reduced temperature, namely we solve Eqs. (10), (11) and (12) for both MFT and EFT by combining the numerical methods of Adams–Moulton predictor corrector with the Romberg integration. This study leads us to characterize the nature (continuous or discontinuous) of transitions as well as to obtain the DPT points. In order to see the F+P mixed phase, we present thermal behaviour of the order parameter for EFT as seen in Fig. 2. Figures 2(a) and 2(b) illustrate the thermal variations of Q, A/zJ and C/zJ for $\omega = 1.0$, $h/zJ = 0.65$ and $z = 4$ in the cases of two different initial values, i.e. $M = 1$ for Fig. 2(a), and $M = 0$ for Fig. 2(b). In Figs. 2(a) and 2(b), $T_{\rm C}$ is the second-order phase transition temperature from F phase to P phase, and $T_{\rm t}$ is the first-order phase transition temperature from P phase to F phase. In Fig. 2(a), $Q = 1$ at zero temperature, and it decreases to zero continuously as the reduced temperature increases, therefore a second-order phase transition occurs from F phase to P phase at $T_{\rm C} = 0.2725$. In Fig. 2(b), $Q = 0$ at zero temperature, the system undergoes two successive phase transitions as the temperature increases: the one is a first-order phase transition, because discontinuities occur for the dynamic magnetization, the hysteresis loop area and the correlation, and the transition is from P phase to F phase at $T_{\rm t} = 0.0275$; the other is the second-order phase transition from F phase to P phase at $T_{\rm C} = 0.2725$. From Figs. 2(a) and 2(b), one can see that the F+P mixed phase exists in the system and this fact is seen in the phase diagram of Fig. 3(b), explicitly. Ma and Wang[25] classified these phase transitions as follows: A second-order (continuous) as type I, a first-order (jump or discontinuous) as type II and mixed transition as type III while developing the dynamic phase transition theory.

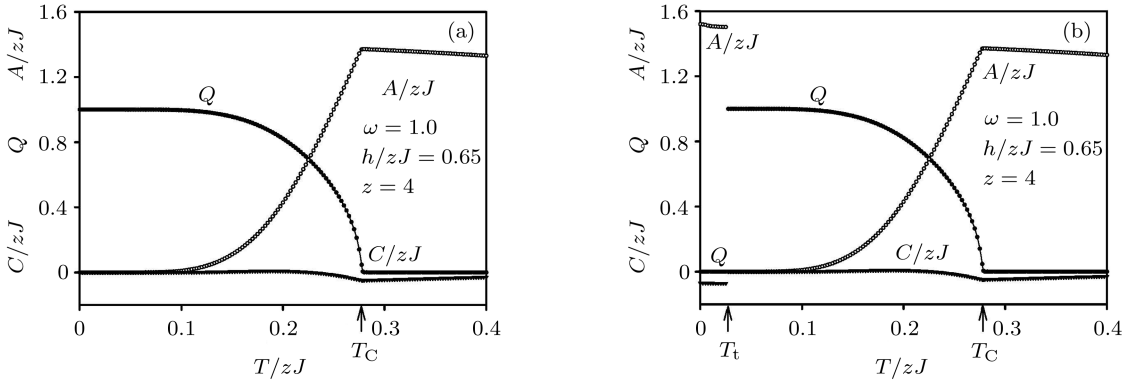


Fig. 2. Thermal behaviours of the Q, C/zJ and A/zJ for the values of $\omega = 1.0$, $h/zJ = 0.65$ and $z = 4$, where the •, ∘ and ▲ lines are for Q, C/zJ and A/zJ, respectively; $T_{\rm C}$ is the second-order phase transition temperature from F phase to P phase; $T_{\rm t}$ is the first-order phase transition temperature from P phase to F phase. Panel (a) exhibits a second-order phase transition from ferromagnetic (F) phase to P phase for $\omega = 1.0$, $h/zJ = 0.65$ and $z = 4$, and the initial value of $M = 1$; $T_{\rm C}$ is found to be 0.2775. Panel (b) shows two successive phase transitions: the first one is a first-order phase transition from P phase to F phase and the second one is a second-order phase transition from F phase to P phase for $\omega = 1.0$, $h/zJ = 0.65$ and $z = 4$, and the initial values of $M = 0$; $T_{\rm t}$ and $T_{\rm C}$ are found to be 0.0275 and 0.2775 respectively.

We present the dynamic phase diagrams in the $(T/zJ, h/zJ)$ plane in Figs. 3 and 4. In Figs. 3 and 4, the solid and the dash lines represent the second- and first-order phase transition lines, respectively, and the dynamic tricritical point is denoted by a solid circle. Figure 3 (a) represents the phase diagram for $\omega = 0.5$ within both theories. In this phase diagram, at high values of T/zJ and h/zJ the solution is paramagnetic and at low values of T/zJ and h/zJ it is ferromagnetic. The boundary between these regions, F $\rightarrow$ P, is represented by the second-order phase line for the MFT and the EFT separately. At low values of T/zJ, there is a range of values of h/zJ in which P and F phases or regions coexist, called the coexistence region or mixed phase, F+P

only within the EFT. The F+P phase is separated from the F and the P phases by the first-order phase lines. The system also exhibits only one dynamic tricritical point where both first-order phase transition lines merge and signal the change from the first- to the second-order phase transitions. Moreover, the tricritical point also occurs for the MFT calculation, which occurs for the low values of h/zJ and high values of T/zJ.

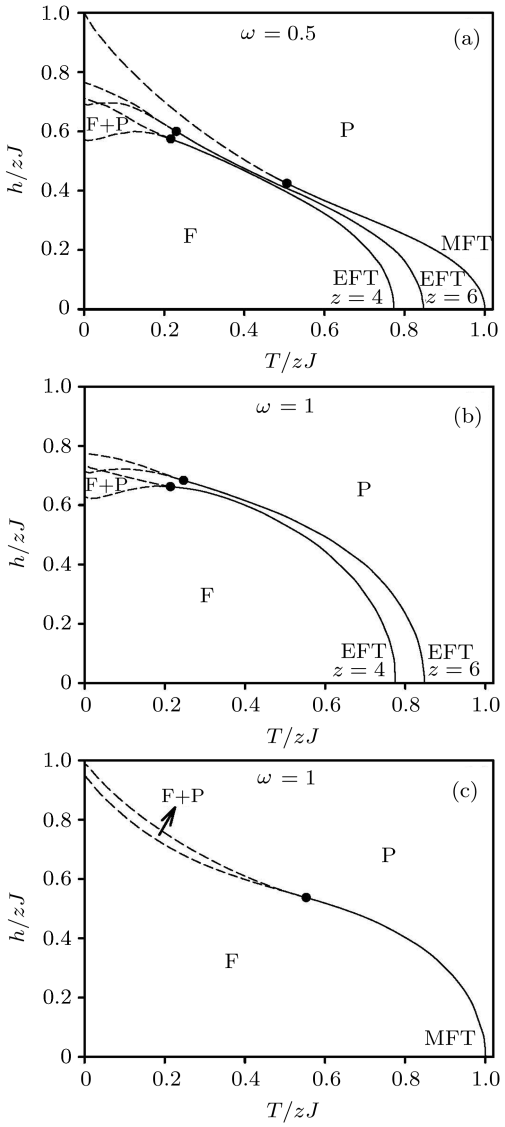


Fig. 3. Dynamic phase diagrams in the (T/zJ, h/zJ) plane for three different vales of ω: (a) 0.5 for both EFT and MFT, (b) 1.0 for the EFT and (c) 1.0 for the MFT P phase F phase, and F+P are found. Dash and solid lines represent the first- and second-order phase transitions, respectively and the dynamic tricritical points are indicated with solid circle.

Figures 3(b) and 3(c) show the calculated results within the EFT and the MFT, respectively for $\omega = 1.0$. The behaviours of these phase diagrams are similar to these in Fig. 3(a) for the EFT calculation; hence the F+P phase also exists for MFT, contrary to the result of Shi *et al.*[1] Figure 4 is for the case of $w = 2\pi$ ($\Omega/2\pi = 1$ is the notation of Tomé and de Oliveira[2]). We have presented this figure to show that our result for the MFT is exactly the same as Tomé and de Oliveira's[2] result (see the comparison between this figure and Fig. 6 in Ref. [2]).

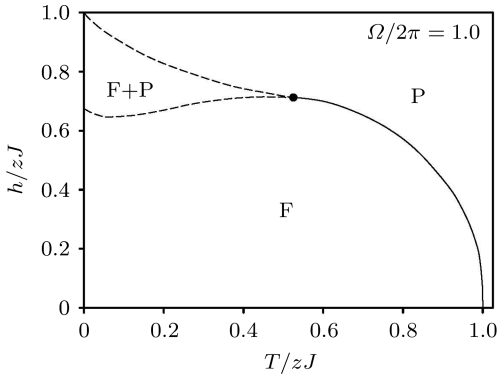


Fig. 4. The same as the description of Fig. 3, but for $\Omega/2\pi = 1$ that is the notation of Tomé and de Oliveira.[2]

Finally, in order to see the influence of the external magnetic field frequency (ω) and static magnetic field amplitude (h_0) for both MFT and EFT, we have performed the calculations for different external field frequencies and static fields.

Figures 5(a) and 5(b) show the thermal variations of the dynamic magnetization (Q), hysteresis loop area (A/zJ) and correlation (C/zJ) for three different values of the magnetic field frequency (ω) and $h/zJ = 1.0$ for the MFT and EFT on square lattice $z = 4$, respectively. In both cases, it is observed that near the dynamic phase transition point, the dynamic correlation gives a shallow dip, and the hysteresis loop area shows a peak above the dynamic phase transition point, which is consistent with the EFT[1] and Monte Carlo results.[5] From these figures, we find that the transition temperatures become small when ω is small. Moreover, when the ω is big, the values of A/zJ and C/zJ at the transition temperatures are small. Here, it is also clear that the temperature dependence of the hysteresis loop area is assumed to be different functions for the $Q > 0$ states for lower temperatures and $Q = 0$ states for higher temperatures. These different functions are separated by the dynamic critical point, and the first-order derivative, $\partial A/\partial T$, is not continuous at the dynamic critical point. Therefore, the temperature dependence is a piecewise analytic function.

Figures 6(a) and 6(b) illustrate the thermal variations of Q for several values of static field amplitudes h_0 for the MFT and EFT on the square lattice $z = 4$, respectively. These figures indicate that the system does not undergo any phase transition. These behaviours are similar to those in Fig. 6(a) of Ref. [8] and Fig. 3 of Ref. [14].

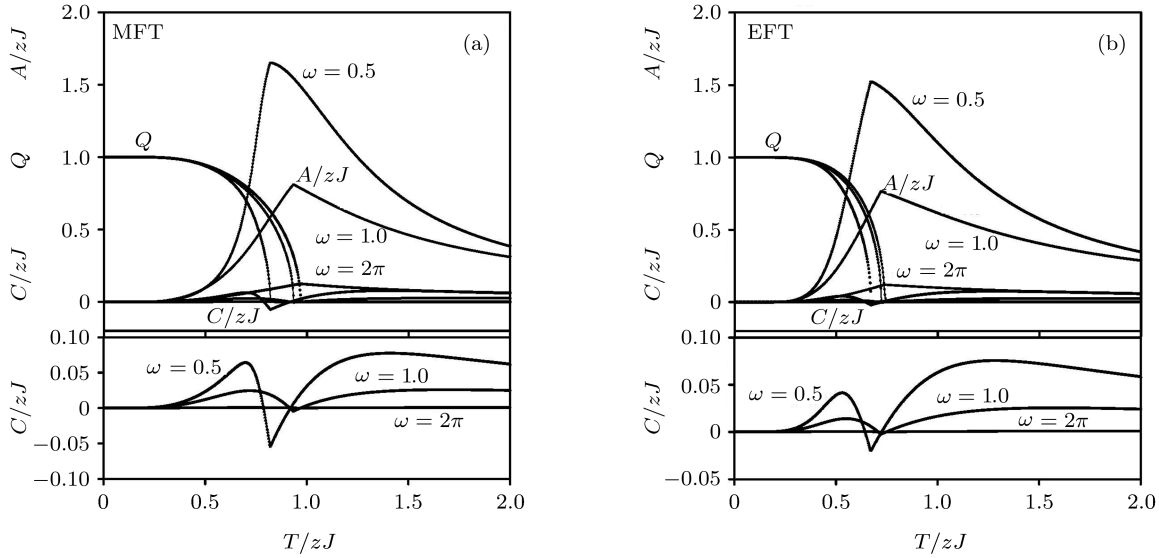


Fig. 5. Thermal variations of dynamic magnetization (Q), hysteresis loop area (A/zJ) and correlation (C/zJ) for three different values of the magnetic field frequency ($\omega = 0.5$, 1.0, 2π) and $h/zJ = 1.0$. Panel (a) is for the MFT, and panel (b) if for the EFT on square lattice $z = 4$.

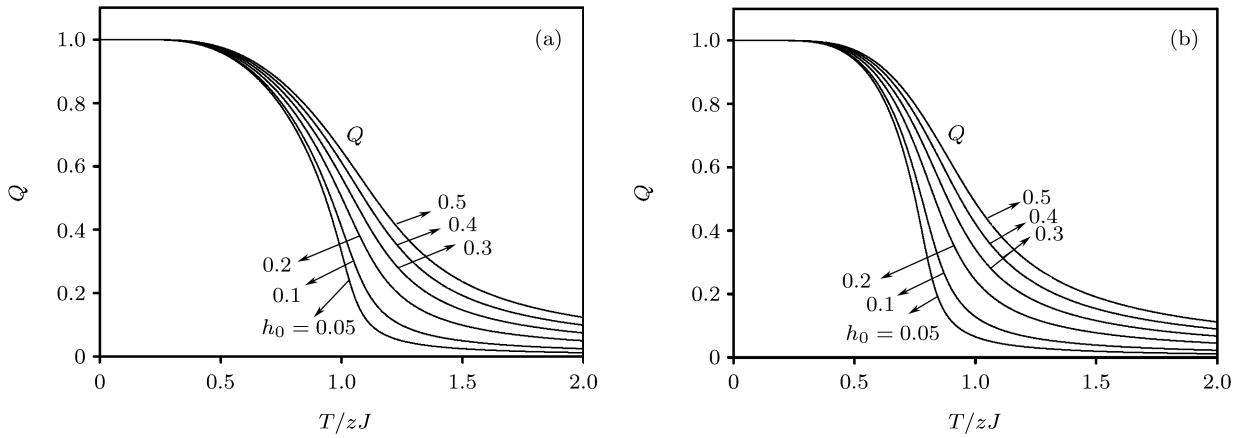


Fig. 6. Thermal variations of dynamic magnetization (Q) for several values of the static external field amplitude h_0. Panel (a) is for the MFT and panel (b) is for the EFT on square lattice $z = 4$.

In summary, the dynamic magnetization, the hysteresis loop area, and the dynamic correlation have been calculated separately (both from MFT and EFT) and studied each as a function of temperature. In both cases, it is observed that the dynamic correlation shows a shallow dip near the phase transition point. The dynamic phase transition point has been identified as the minimum-correlation point.[7] The hysteresis loop area becomes maximum above the dynamic phase transition point. We also present the complete dynamic phase diagrams within the MFT and EFT with correlations. We find that the dynamic phase diagrams for the MFT are exactly the same as those in the earlier work of Tomé and de Oliveira[2] and the results of the EFT are similar to those of the MFT, except following two differences: (1) The F+P phase does always appear for all ω values; hence the dynamic phase diagrams that were presented by Shi *et*

al.[1] are incomplete within both theories, except for $\omega \leq 0.60$ within the MFT. This fact can easily be seen from Fig. 3. In Fig. 3(a), the F+P mixed phase always occurs within the EFT, but not within the MFT for $\omega < 0.60$. Moreover, the F+P phase always exists in both MFT and EFT for $\omega \geq 0.60$ as seen in Figs. 3(b) and 3(c). (2) The tricritical point appears at high values of the h/zJ and low values of T/zJ. As Shi *et al.*[1] mentioned, the kinetic Monte Carlo (MC) simulations by Korniss *et al.*[6] show that there is no tricritical point in the infinite-system limit and the tricritical point claimed to be found in MC simulations by Acharyya[5] is, in fact, due to a finite-size effect. The EFT results thus go some way toward correcting the kinetic MFT result, but they do not introduce sufficiently strong fluctuations to the obtained the correct result: the microscopic model does not have a dynamic tricritical point in the infinite-system limit. Moreover, we also investigate the influence of the external field frequency (ω) and static external field amplitude (h_0) for both MFT and EFT calculations. We find that the behaviour of the system strongly depends on values of ω and h_0.

Acknowledgements

One of authors (B.D.) would like to express his gratitude to the TÜBİTAK for the Ph.D scholarship.

Appendix

The coefficients a_i ($i = 0, 1, \ldots, 4$) in Eq. (8) and b_j ($j = 0, 1, \ldots, 6$) in Eq. (9) can be easily calculated by using the mathematical relation $\exp(\alpha \nabla)\ f(x) = f(x + \alpha)$, where $\nabla = \partial/\partial x$ is a differential operator. These coefficients a_i ($i = 0, 1, \ldots, 4$) and b_j ($j = 0, 1, \ldots 6$) are obtained as follows:

$$a_0=\frac{1}{16}\left[f(h+4J)+4f(h+2J)+6\,f(h)+4f(h-2J)+f(h-4J)\right],$$

$$a_1=\frac{1}{4}\left[f(h+4J)+2f(h+2J)-2f(h-2J)-f(h-4J)\right],$$

$$a_2=\frac{3}{8}\left[f(h+4J)-2\,f(h)+f(h-4J)\right],$$

$$a_3=\frac{1}{4}\left[f(h+4J)-2f(h+2J)+2f(h-2J)-f(h-4J)\right],$$

$$a_4=\frac{1}{16}\left[f(h+4J)-4f(h+2J)+6\,f(h)-4f(h-2J)+f(h-4J)\right],$$

$$b_0=\frac{1}{64}\left[f\,(h+6J)+6f\,(h+4J)+15f\,(h+2J)+20f\,(h)+15f\,(h-2J)+6f\,(h-4J)+f\,(h-6J)\right],$$

$$b_1=\frac{3}{32}\left[f\,(h+6J)+4f\,(h+4J)+5f\,(h+2J)-5f\,(h-2J)-4f\,(h-4J)-f\,(h-6J)\right],$$

$$b_2=\frac{15}{64}\left[f\,(h+6J)+2f\,(h+4J)-f\,(h+2J)-4f\,(h)-f\,(h-2J)+2f\,(h-4J)+f\,(h-6J)\right],$$

$$b_3=\frac{5}{16}\left[f\,(h+6J)-3f\,(h+2J)+3f\,(h-2J)-f\,(h-6J)\right],$$

$$b_4=\frac{15}{64}\left[f\,(h+6J)-2f\,(h+4J)-f\,(h+2J)+4f\,(h)-f\,(h-2J)-2f\,(h-4J)+f\,(h-6J)\right],$$

$$b_5=\frac{3}{32}\left[f\,(h+6J)-4f\,(h+4J)+5f\,(h+2J)-5f\,(h-2J)+4f\,(h-4J)-f\,(h-6J)\right],$$

$$b_6=\frac{1}{64}\left[f\,(h+6J)-6f\,(h+4J)+15f\,(h+2J)-20f\,(h)+15f\,(h-2J)-6f\,(h-4J)+f\,(h-6J)\right].$$

References

[1] Shi X, Wei G and Li L 2008 *Phys. Lett.* A **372** 5922
[2] Tomé T and de Oliveira M J 1990 *Phys. Rev.* A **41** 4251
[3] Buendía G M and Machado E 1998 *Phys. Rev.* E **58** 1260
[4] Chakrabarti B K and Acharyya M 1999 *Rev. Mod. Phys.* **71** 847
[5] Acharyya M 1999 *Phys. Rev.* E **59** 218
[6] Korniss G, Rikvold P A and Novotny M A 2002 *Phys. Rev.* E **66** 056127
[7] Acharyya M 1998 *Phys. Rev.* E **58** 179
[8] Keskin M, Canko O and Temizer Ü 2005 *Phys. Rev.* E **72** 036125
[9] Keskin M, Canko O and Deviren B 2006 *Phys. Rev.* E **74** 011110

[10] Robb D T, Rikvold P A, Berger A and Novotny M A 2007 *Phys. Rev.* E **76** 021124
[11] Kim B J and Hong H 2008 *J. Korean Phys. Soc.* **52** 203
[12] Keskin M, Kantar E and Canko O 2008 *Phys. Rev.* E **77** 051130
[13] Oh S K and Kang H J 2008 *J. Korean Phys. Soc.* **47** 6
[14] Deviren B, Keskin M and Canko O 2009 *J. Magn. Magn. Mater.* **321** 458
[15] Samoilenko Z A, Okunev V D, Pushenko E I, Isaev V A, Gierlowski P, Kolwas K and Lewandowski S J 2003 *Inorganic Materials* **39** 836
[16] Gedik N, Yang D S, Logvenov G, Bozovic I and Zewail A H 2007 *Science* **316** 425
[17] Kanuga K and Çakmak M 2007 *Polymer* **48** 7176
[18] Robb D T, Xu Y H, Hellwig O, McCord J, Berger A, Novotny M A and Rikvold P A 2008 *Phys. Rev.* B **78** 134422
[19] Honmura R and Kaneyoshi T 1979 *J. Phys.* C: *Solid State Phys.* **12** 3979
[20] Kaneyoshi T, Fittipaldi I P, Honmura R and Manabe T 1981 *Phys. Rev.* B **24** 481
[21] Kaneyoshi T and Beyer H 1980 *J. Phys. Soc. Japan* **49** 1306
[22] Kaneyoshi T, Honmura R, Tamura I and Sarmento E F 1984 *Phys. Rev.* B **29** 5121
[23] Zernike F 1940 *Physica* **7** 565
[24] Kaneyoshi T 1986 *Phys. Rev.* B **33** 7688
[25] Ma T and Wang S 2005 *World Scientific Series on Nonlinear Science* Series A: *Monograps and Treaties* 53 (Hackensack: World Scientific Publishing)
Ma T and Wang S 2007 *Stability and Bifurcation of Nonlinear Evolutions Equations* (Beijing: Science Press) (in Chinese)
Ma T and Wang S 2008 *J. Math. Phys.* **49** 053506